Tellus (2003), 55A, 193–207
Printed in UK. All rights reserved

TELLUS
ISSN 0280–6495

The atmospheric response to North Atlantic SST anomalies in seasonal prediction experiments

By HAI LIN* and JACQUES DEROME, *Department of Atmospheric and Oceanic Sciences and Centre for Climate and Global Change Research, McGill University, 805 Sherbrooke Street West, Montréal, Québec H3A 2K6, Canada*

(Manuscript received 4 December 2001; in final form 26 September 2002)

ABSTRACT

Seasonal forecasts performed over a 26 yr period as part of the Historical Seasonal Forecasting Project (HFP) are used to analyze the influence of North Atlantic sea surface temperature (SST) anomalies on the atmospheric circulation, its seasonality, and model dependence. The signals related to the El Niño events are first removed from both the SST and the atmospheric data. The North Atlantic SST and the ensemble mean forecast are then correlated over the 26 yr to identify the model response to the SST forcing. The signal-to-noise ratio shows that in spring there is a significant forecast signal that is related to the SST anomaly in the North Atlantic. In that season the two models used in the HFP yield responses to the SST anomaly that are both similar to each other and to the observed response. For the other seasons the agreement between the responses and the observed atmospheric anomalies is poor. In winter the response is very sensitive to the model used.

1. Introduction

Predictions beyond about one month depend largely on signals in the atmospheric variability that are forced by anomalies in the lower boundary conditions, such as the sea surface temperature (SST) and sea ice coverage. One remarkable extratropical signal corresponding to a sea surface temperature increase (decrease) in the equatorial eastern Pacific in an El Niño (La Niña) year is the Pacific/North American (PNA) teleconnection pattern. The latter takes the form of below-normal (above-normal) geopotential heights in the North Pacific and the south-eastern United States and above-normal (below-normal) heights centered over Hawaii and western Canada (Horel and Wallace, 1981). This linkage between the tropical SST anomalies and the PNA pattern is supported by modeling studies (e.g. Lau and Nath, 1994) and Rossby wave energy dispersion theory (Hoskinsand Karoly, 1981; Branstator, 1985). The signal is relatively strong and can benefit seasonal forecasts (Kumar and Hoerling, 1995; Derome et al., 2001).

There is also strong interannual variability in the midlatitude SSTs (e.g. Kushnir, 1994). Observational studies indicate that the latter are generated largely by atmospheric variability through fluctuations in the surface wind, temperature and humidity (e.g. Cayan, 1992). One evidence for this is the observation that the correlation between the atmospheric and oceanic temperatures is found to be the strongest when the atmosphere leads the ocean by 2–3 wk (Deser and Timlin, 1997). On the other hand, the extent to which mid-latitude SST anomalies feedback to affect the atmospheric circulation is of great interest, since such a feedback could contribute to some atmospheric predictability. As the oceans have a relatively large heat capacity and thermal inertia, SST anomalies have decay time scales of the order of months (Frankignoul, 1985), which is longer than the predictability limit of the unforced atmospheric flow. Evidence for the existence of a detectable feedback was provided, in particular, by Czaja and Frankignoul (1999).

*Corresponding author.
e-mail: hai.lin@mcgill.ca

Numerical modeling studies of the atmospheric response to mid-latitude SST anomalies have often yielded conflicting results. The atmospheric responses differ not only in magnitude but also in structure. For example, with similar SST anomalies, Palmer and Sun (1985) find a significant response with a barotropic structure, while Kushnir and Held (1996) find a response that is shallow and baroclinic. Some authors obtain significant nonlinearity in the response to mid-latitude SST anomalies (Pitcher, 1988; Kushnir and Lau, 1992), while others find that the response to a cold SST anomaly is the opposite of the response to a warm SST anomaly (Ferranti et al., 1994). Lau and Nath (1990) find that midlatitude SST anomalies play a significant role in generating wintertime interannual variability, while in another study (Lau and Nath, 1994) the result is found to be not reproducible with a slightly different version of the same GCM. Finally, Peng et al. (1995; 1997) find that the response depends on the time of year. A review of previous studies on the atmospheric response to extra-tropical SST anomalies was given by Robinson (2000). There are also diagnostic and modeling studies which suggest a possible influence on seasonal atmospheric fluctuations by tropical Atlantic SSTs (e.g. Robertson et al., 2000; Cassou and Terray, 2001).

A variety of factors may contribute to the differences in the results of the model experiments. Firstly, the response is weak and embedded in a vigorously turbulent atmosphere, i.e. the signal to noise ratio is low. Large ensembles of experiments may be needed to extract the signal. Differences in model resolution and the ability to resolve transient eddies and their feedbacks may be another factor (Kushnir and Held, 1996). Peng and Whitaker (1999) suggest that the sensitivity of the eddy forcing to the background flow may explain the difference of the responses in two different months. Using a simple general circulation model, Hall et al. (2001) showed how the atmospheric response is influenced by a variety of factors, such as the position of the SST anomaly with respect to the upper level jet.

The Canadian Climate Variability Research Group (now the Canadian Climate Variability Research Network) has conducted a project termed the Historical Seasonal Forecasting Project (HFP). The goal was to test over a 26 yr period the skill of two global atmospheric circulation models in predicting seasonal-mean atmospheric conditions. Studies such as that by Zwiers (1996) had looked at the potential predictability of the atmosphere, i.e. the predictability level that can be achieved in a perfect model context when the SST and sea ice conditions are assumed known. In the HFP an operational forecasting environment was mimicked in that the SST and sea ice conditions were not assumed known at the start of the seasonal forecasts, and the latter were verified against observations. Starting from the beginning of each season, a set of six seasonal predictions were performed with slightly different initial conditions. During the three-month integrations, persistent SST anomalies were specified as those of the previous month and added to a monthly varying climatological SST field. Two numerical models were used to perform the seasonal predictions with the same setup. For each of the four seasons, ensembles of six forecasts were produced with each model for the 26 yr in the period from December 1969 to February 1995. Some results of the HFP, particularly those related to SST variability in the tropical Pacific, are described in Derome et al. (2001).

Because the SST anomalies are specified during the seasonal predictions in the HFP, the predictions provide a significant database (2 models $\times$ 6 ensemble members $\times$ 4 seasons $\times$ 26 yr $=$ 1248 experiments) to analyze the relationship between the atmosphere and the SST anomalies in these two models. In this paper we focus on the atmospheric response to SST anomalies in the North Atlantic, its seasonality and dependence on models.

The paper is structured as follows. In section 2, we briefly introduce the HFP project and the data used in this study. In section 3, the leading mode of interannual Atlantic SST variability is identified for the four seasons. In section 4, we calculate the variance of the atmospheric signal that is related to the leading mode of Atlantic SST variability, and identify the areas with a large signal-to-noise (S/N) ratio. In section 5, we present the model and observed atmospheric structures that are related to this leading mode of North Atlantic SST anomaly. Comparisons are made for the two models and for the four seasons. Conclusions and discussions follow in section 6.

2. The Historical Seasonal Forecasting Project (HFP) and data

2.1. The Historical Forecasting Project (HFP)

A detailed description of the HFP is given by Derome et al. (2001), so only the hightlights will be given here. Three-month forecasts were produced for the period January 1969 to Febuary 1995 with the

second generation of a General Circulation Model (GCM2 thereafter) developed at the Canadian Centre for Climate Modelling and Analysis (CCCma) for climate studies, as well as with a reduced-resolution version of the global spectral model (SEF thereafter) developed at Recherche en Prévision Numérique (RPN) for numerical weather prediction purposes.

The GCM2 has been used for a number of climate simulation studies (e.g. Boer et al., 1984; McFarlane et al., 1992) that describe its formulation in detail. It is a global spectral model with a triangular 32 (T32) horizontal resolution and 10 levels in the vertical. The SEF has been used in previous studies on global data assimilation and medium-range weather forecasting (Ritchie, 1991; Ritchie and Beaudoin, 1994). It is also a global spectral model, but with a T63 horizontal resolution and 23 levels.

Three-month predictions were made for each season of the 26 yr, winter being defined as December, January and Febuary (DJF), spring as March, April and May (MAM), summer as June, July and August (JJA), and fall as September, October and November (SON). The reanalysis dataset from the National Centers for Environmental Predictions (NCEP) and the National Center for Atmospheric Research (NCAR) (Kalnay et al., 1996) was used for the initial conditions of the 3-month forecasts. The initial conditions for the six ensemble members of each model were taken from the reanalysis dataset at lags of 6 h just previous to the start of the season. During the forecast the global SST field is specified as the monthly SST anomaly of the month prior to the forecast period plus a monthly-varying climatological SST field. The SSTs are taken from the GISST2.2 dataset (Rayner et al., 1996). There are some differences in the treatment of sea ice, snow cover and soil conditions in the two models as described by Derome et al. (2001).

2.2. The data used

The data used in this study include: (a) monthly mean global SST fields from the GISST2.2 dataset over the 26 yr of the HFP, (b) the seasonal-mean 500 hPa geopotential height, the 700 hPa temperature and mean sea level pressure from the NCEP/NCAR reanalyses and (c) the same variables as in (b) but from the ensemble-mean of the forecasts produced by the GCM2 and SEF models. The seasonal means refer to the averages over DJF, MAM, JJA and SON.

2.3. Data pre-filtering: removing the trend and the El Niño signal

To concentrate on the interannual time scale we first remove the long-term linear trend from the data at each grid point using a least-square method. As we are interested in isolating the atmospheric response that is related to the North Atlantic SST variability, we then remove from the data the variability that is linearly related to the El Niño signal. This is done by first performing an empirical orthogonal function (EOF) analysis on the SST data (monthly-mean or seasonal-mean) over the tropical Pacific region (40°S–40°N, 120°E–90°W). The first EOF, regardless of month or season, is found to explain about 30% of the SST variance in that region. The principal component (PC) of that first mode is then regressed against the data to be filtered at every grid point in space, and the resulting global "El Niño signal" is subtracted from the data. This process is also applied to the NCEP data used for comparison with the model. Except where noted otherwise, the PC of the SST and the data to be filtered are synchronous (same month or same season). It should be understood that, except where noted explicitly, all the results presented in what follows were obtained with pre-filtered data.

3. SST anomalies in the North Atlantic

In the HFP, the SST anomaly is specified during the entire season to be that observed during the month preceding the season being forecast, i.e. SST anomalies in Febuary, May, August and November are used for MAM, JJA, SON and DJF forecasts, respectively. In this section we will identify the leading mode of the interannual variability of SST in the North Atlantic for each of the four months through an EOF analysis over the region of 0–80°N, 0–90°W. The effect of unequal areas represented by different grid points is taken into account by multiplying the monthly-mean SST by the square root of the cosine of the latitude at that grid point.

Figures 1a, b, c and d show the linear regression patterns of the monthly-mean SST to the PC of the leading SST mode in the North Atlantic for February, May, August and November, respectively. The magnitude represents the SST anomaly in K corresponding to one standard deviation of the PC of the leading mode in the EOF. As can be seen, for both February and May, the leading mode of the interannual variablity in the North Atlantic SST anomaly is a tripole pattern as

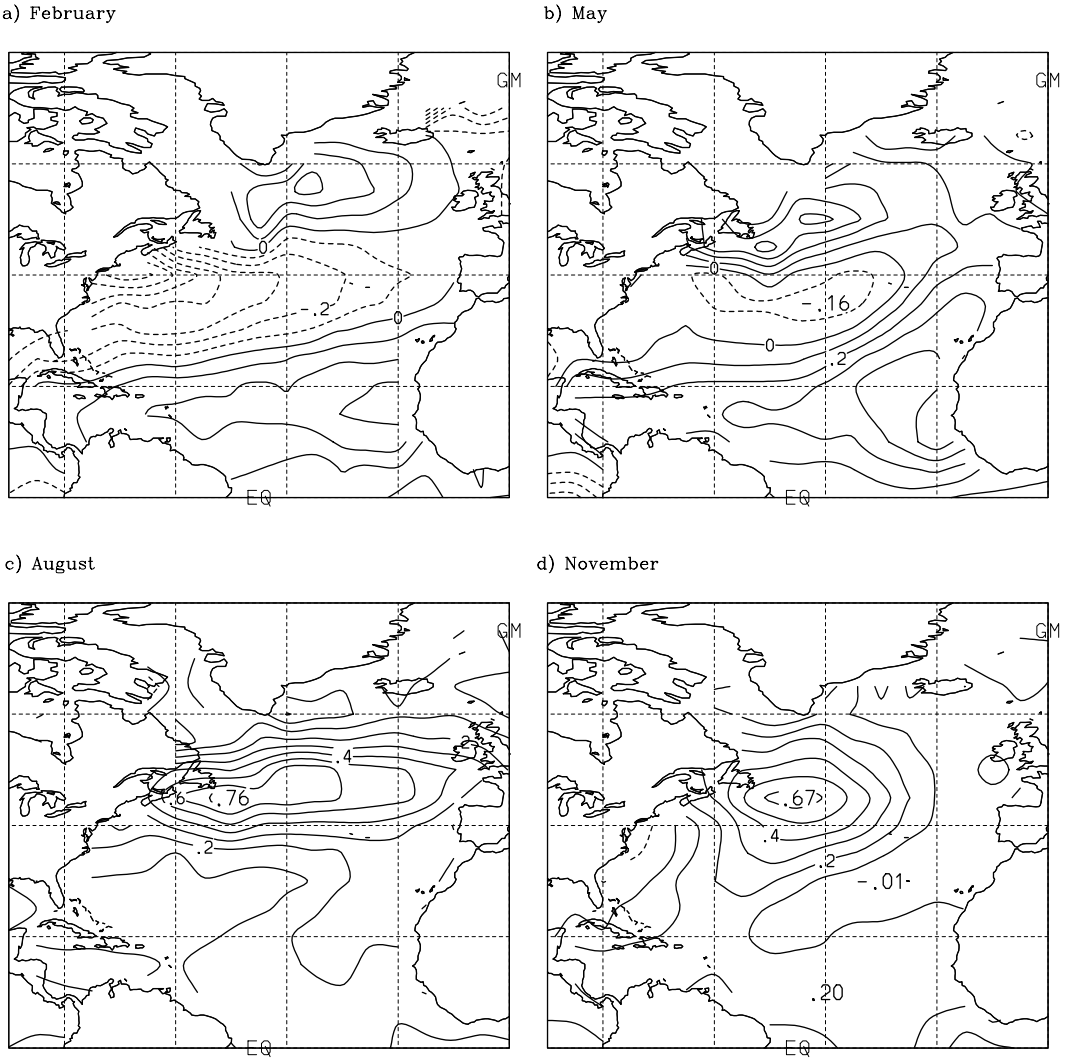

Fig. 1. Linear regression pattern of the monthly mean SST to the leading principal component of SST in the North Atlantic for (a) February, (b) May, (c) August and (d) November. The contour interval is 0.1°. Negative values are indicated by dashed lines.

observed in previous studies (e.g. Kushnir, 1994). For August and November, the pattern is more like a monopole, centered in the midlatitude North Atlantic.

4. The atmospheric signal related to the North Atlantic SST variability

Given a large ensemble of seasonal-mean forecasts, for a given season, over many years, the interannual variability in the ensemble mean represents the variability in the signal that is related to the external forcing by the SST anomalies. While in our case the ensembles of six members cannot be considered large, we will use the ensemble mean as an estimate of the SST-forced anomaly. To identify the signal in the forecasts that is related to the variability of the leading SST mode in the North Atlantic, the ensemble-averaged seasonal-mean of the predicted 500 hPa geopotential height field is linearly regressed against the PC

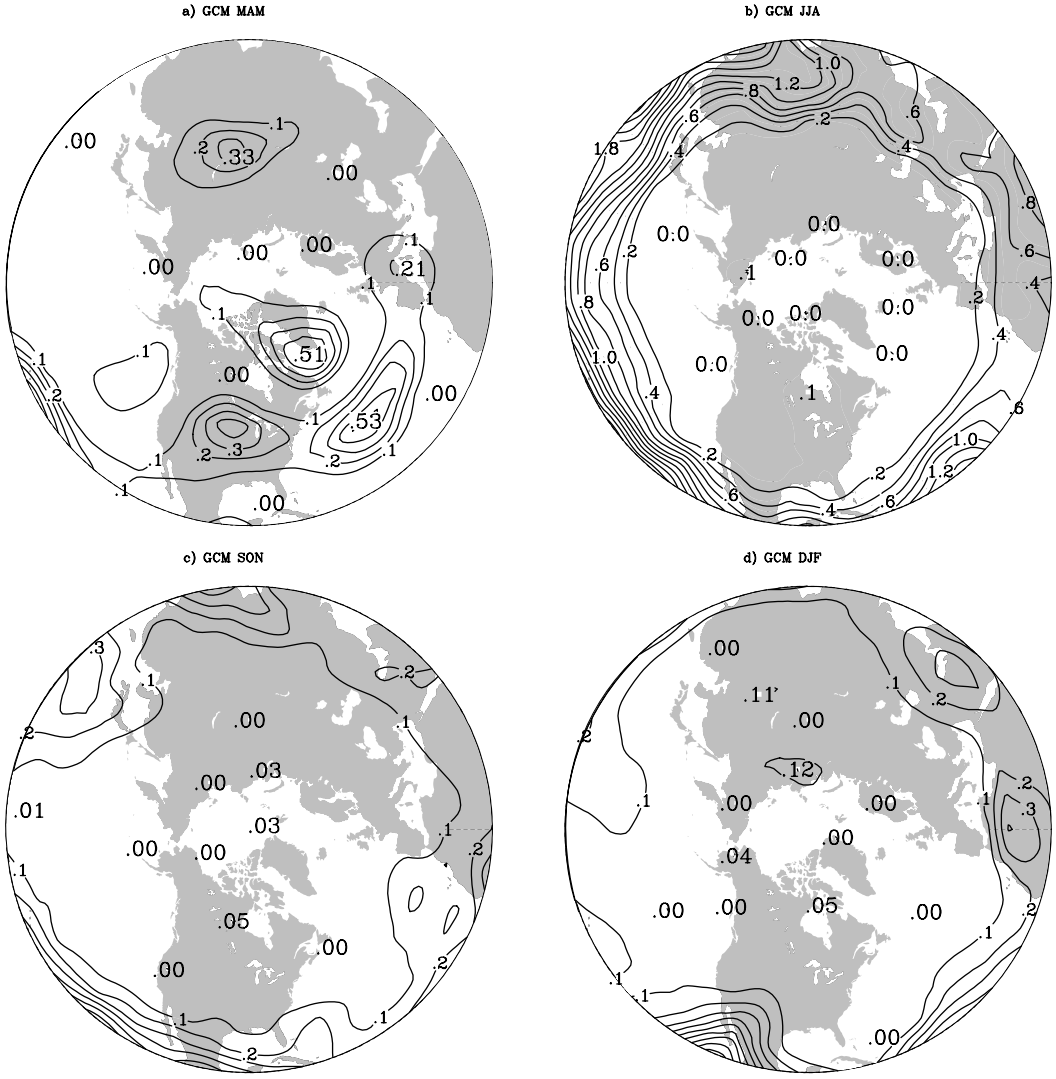

Fig. 2. Signal-to-noise ratio for GCM for (a) MAM, (b) JJA, (c)SON and (d) DJF. The contour interval is 0.1.

of the first SST mode of the previous month in the North Atlantic. The signal variance is calculated as the square of the regression averaged over 26 yr, separately for each season and each model. The noise variance is obtained as the inter-member variance for the model and season under study averaged over the 26 yr. The S/N ratio is then the ratio of these two variances.

Figures 2 and 3 show the S/N ratio for the GCM2 and SEF models, respectively. Both models show similar features for spring, summer and fall. In spring, two centers of high S/N ratio can be found in the North Atlantic area, one near Greenland and the other over the central Atlantic, with a maximum ratio of about 0.5. This is the only season with a significant S/N ratio in this region. In summer and fall, the main signals are in the low latitudes, and the signal in the middle and high latitudes is negligible compared to the noise. In winter, the two models give different S/N ratio distributions. The GCM2 shows little notable signal in the extratropics, while the SEF has a train of centers from Eurasia to the North Pacific.

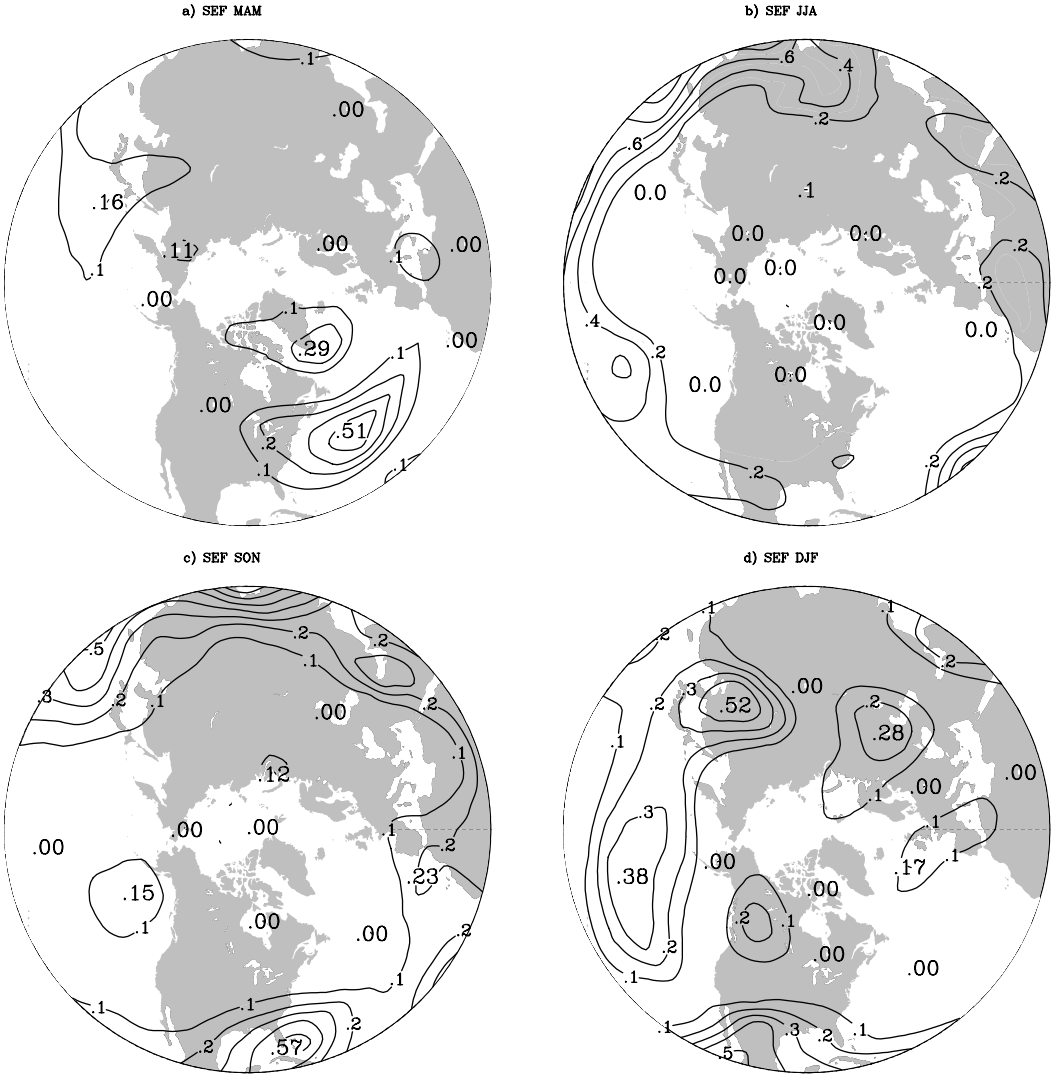

Fig. 3. As Fig. 2 except for SEF.

It is an open question why the SEF alone has these centers of larger S/N ratio so far away from the North Atlantic. Model deficiencies may be to blame, as could the relatively small ensemble of six members available to estimate the S/N ratio. On the other hand, it will be seen later (Fig. 9) that the NCEP DJF data (as well as the SEF ensemble mean) has a statistically significant signal over eastern Asia and the North Pacific associated with the first EOF of Atlantic SST. So the possibility remains that the maxima seen in Fig. 3 in these regions is meaningful.

5. The North Atlantic SST anomalies and the associated atmospheric circulations

A correspondence between the leading mode of the North Atlantic SST and the atmospheric anomalies during a given season can be established through a linear regression map. Since in the HFP the SST anomaly persists during the forecast season, this correspondence can be viewed as the atmospheric response to the SST anomaly. We have calculated the response in the 500 hPa geopotential height, sea level pressure

and 700 hPa temperature. Due to the highly barotropic vertical structure in the response, in the following discussion we will focus on the 500 hPa geopotential height.

In the following we will show the atmospheric circulation for each season associated with the specified SST anomalies is identified by its leading mode in the North Atlantic. Results for the two models will be compared to each other as well as to the observations. The observed data are represented by the NCEP/NCAR reanalyses, and the predictions are from the six-member ensemble-mean forecasts of the GCM2 and SEF models.

5.1. Spring

Figure 4a shows the linear regression of the GCM2 ensemble-mean and seasonal-mean forecast 500 hPa geopotential height anomaly in spring (MAM) against the PC of the leading mode of the Atlantic SST anomaly in February (Fig. 1a). The values on the map represent the MAM seasonal mean 500 hPa geopotential height anomaly associated with the SST anomaly forcing having the pattern and amplitude presented in Fig. 1a. In the following we will refer to the above as the "Atlantic signal". The shaded areas represent those regressions with a significance level of 0.05 or better. The latter was estimated by a Monte Carlo simulation, in which 500 regressions were computed for each grid point between the time series of the leading mode PC of the Atlantic SST anomaly and the randomized time series of the height anomalies. Significant positive regression values are observed near Greenland and the North Pole, and negative values are found in the midlatitudes from North America to western Europe. The implication is that a positive phase of the North Atlantic SST pattern of Fig. 1a tends to be associated in the GCM2 with a negative phase of the North Atlantic Oscillation (NAO) in the spring season (MAM). With one standard deviation of the SST pattern (a positive SST anomaly of about 0.3° south of Greenland and a negative anomaly of around 0.7° off the east coast of the United States), the seasonal-mean 500 hPa height response is a positive anomaly over Greenland and the North Pole with a maximum of about 18 m and a negative anomaly in the midlatitude North Atlantic with a maximum of about 8 m . The result from the SEF model (Fig. 4b) is very similar to that of the GCM2 over most of the hemisphere, but especially over the North Atlantic, where both models have their maximum S/N ratios (Figs. 2 and 3).

Some studies show that in the real world the midlatitude Atlantic SST forcing and the atmospheric response have a lag of a few months, with the ocean leading. For example, Czaja and Frankignoul (1999; 2002) have used maximum covariance analysis to reveal such statistical relation between atmospheric anomalies and the oceanic forcing. So to estimate how the atmosphere responds to SST anomalies in the North Atlantic in the NCEP/NCAR reanalysis, we computed the regression between the MAM 500 hPa height and the PC of the leading North Atlantic SST mode in February, in the same way as for the models, which allows a 2-month lag between the SST and the mid-month of the atmospheric averaging period. The resulting regression pattern for the observations, shown in Fig. 4c, can be interpreted as the atmospheric anomaly that is associated with the SST pattern of Fig. 1a in February. We see that the atmospheric pattern is similar to that produced by the models over a substantial fraction of the hemisphere, and particularly over the North Atlantic. This strongly suggests that the mode of SST variability shown in Fig. 1a provides some predictability in MAM that the models are able to capture.

We note by inspection of Figs. 4a–c that the atmospheric pattern projects onto the NAO (negative phase), the main mode of variability in the North Atlantic. This is another illustration of a time-mean forced response projecting preferentially onto the main mode of temporal variability, a feature already noted by Hall et al. (2001) and Peng et al. (2002).

To get an idea of the relative importance of the Atlantic signal, we first compute the ratio of its interannual variance to the interannual variance forced by all modes of SST variability (including ENSO), the latter being obtained as the interannual variance of ensemble means. In calculating these variances the average of the two model ensemble means was used (referred as GCMSEF). It should be noted that because the calculations are based on the ensemble means, the internal variability is excluded (to the extent that the 12-member ensemble-mean captures the forced variability). The resulting ratio of the Atlantic signal variance to the "total forced" variance for the MAM 500 hPa height is shown in Fig. 5a. We see that over the western North Atlantic up to a little over 30% of the forced variance is forced by the first mode of Atlantic SST variability. For comparison Fig. 5b shows the corresponding ratio for the El Niño signal. We see that in this case up to a little over 45% of the forced variance is ENSO-related. Not surprisingly, over the North Pacific and northwest North America the ENSO plays a

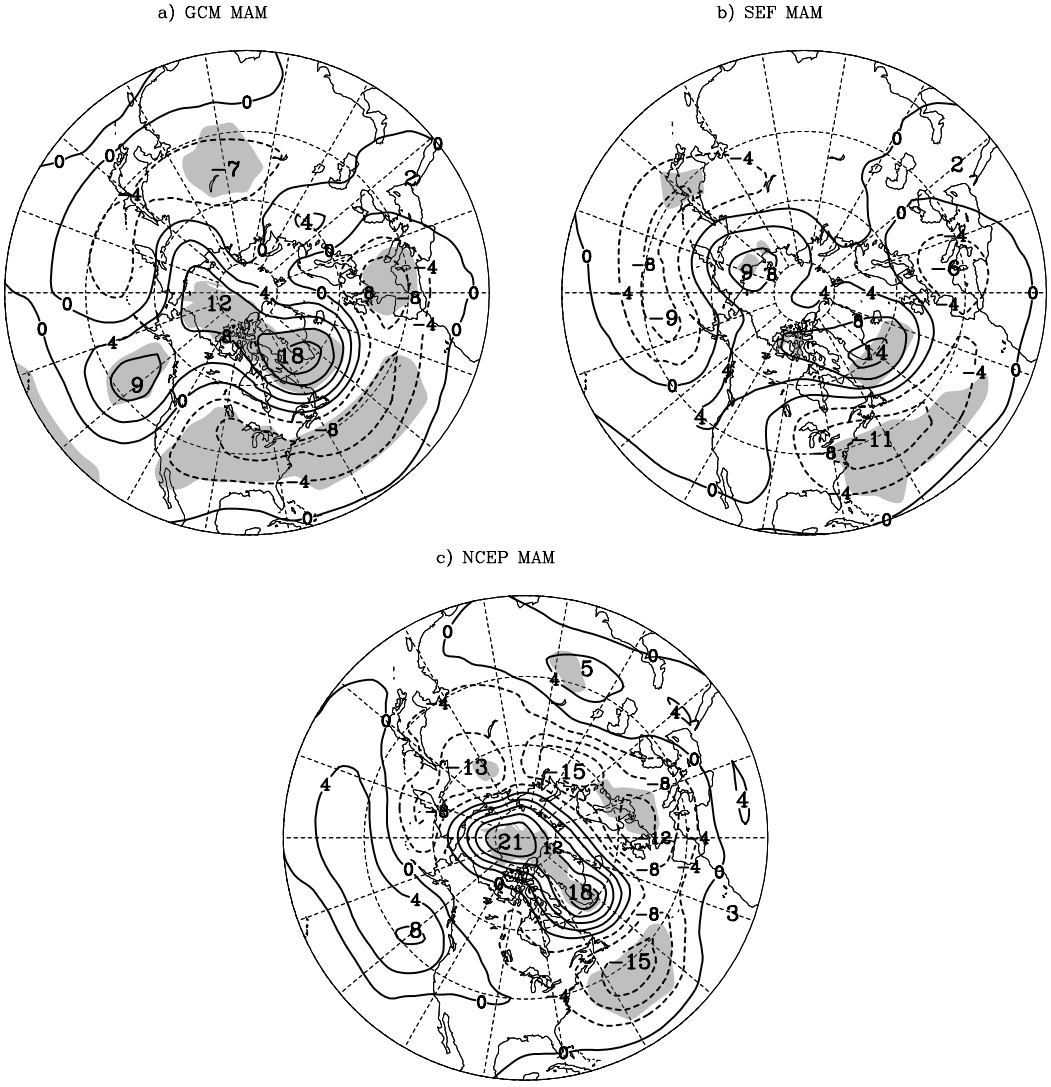

Fig. 4. Linear regression of the seasonal mean 500 hPa geopotential height anomaly in spring (MAM) to the principal component of the leading mode of the Atlantic SST anomaly in February: (a) GCM2 ensemble mean, (b) SEF ensemble mean and (c) NCEP observations. The contour interval is 4 m. The shaded areas represent significance level of 0.05 or better according to a Monte Carlo method.

relatively more important role among forcing agents than the first mode of North Atlantic SST does anywhere, but the latter, with its 30% of forced variance in the western North Atlantic, is nevertheless making a notable contribution.

The total interannual variance in the model simulations can be written as $\sigma_T^2 = \sigma_F^2 + \sigma_I^2 = \sigma_{F1}^2 + \sigma_{FR}^2 + \sigma_I^2$, where σ_F^2 is the variance forced by the SST variability and is obtained from the ensemble means, σ_I^2 is the internal variance, obtained from the inter-member variability, σ_{F1}^2 is the part of the forced variance that is associated with the first mode of Atlantic SST variability, and σ_{FR}^2 is the rest of the SST-forced variance. We will concentrate on the area in the western Atlantic

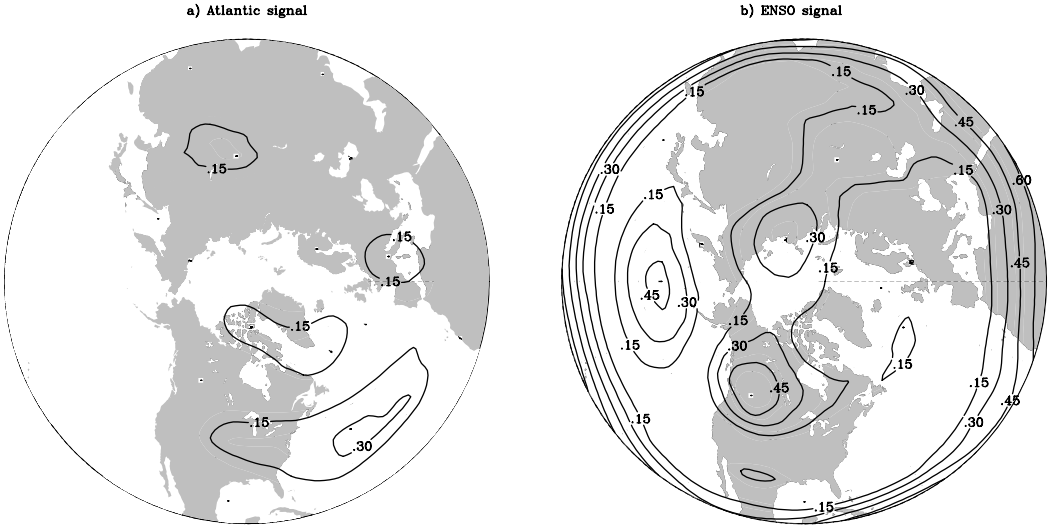

Fig. 5. Ratio of signal variance to the total variance: (a) Atlantic SST signal, (b) El Niño signal.

where the MAM signal to noise ratio is a maximum (Figs. 2a and 3a). From these figures we see that $\sigma_{\mathrm{F1}}^2/\sigma_{\mathrm{I}}^2$ is about 0.52 for either model, while from Fig. 5a we have that $\sigma_{\mathrm{F1}}^2/(\sigma_{\mathrm{F1}}^2 + \sigma_{\mathrm{FR}}^2)$ is about 0.3. This implies that σ_{F1}^2, σ_{FR}^2 and σ_{I}^2 amount to about 16%, 53% and 31%, respectively, of the total variance. In short, the forced variance that is related to the first mode of North Atlantic SST variability accounts for about 16% of the total interannual model variability in MAM conditions in the western North Atlantic.

Peng et al. (2002) found significant nonlinearity in the atmospheric response to their SST anomaly in the North Atlantic in spring. To see if such nonlinearity is present here, composites are computed for the MAM 500 hPa height for the years with positive and negative PC of EOF 1 of February SST. For positive SST PC we have 11 cases, and for negative we have 15 cases. Figure 6 shows the result for GCMSEF. All the main features of one figure are seen in the other, with the sign reversed, as would be expected of a linear response. The amplitude of the response to the positive phase of the SST anomaly (Fig. 1a) is larger than that of the negative phase, a reflection of a nonlinear component to the response.

Since in the HFP the initial condition for each ensemble member is close to the first day of the season, it is possible that persistence of the initial conditions may contribute to the similarity of ensemble members and so lead to an overestimate of the SST forced signal. To see if this is the case and to assess the contribution from the initial conditions, a similar regresion analysis was conducted as in Fig. 4 but with the first month skipped (figure not shown). The resulting patterns are basically as in Fig. 4, but the amplitude is reduced by about 30%, indicating that the main structure shown in Fig. 4 is related to the SST forcing.

5.2. *Summer*

The results corresponding to Fig. 4, but for JJA, are shown in Fig. 7. In this case the May SST pattern of Fig. 1b is used and the atmospheric forecasts and observations are for JJA. For the model responses (Figs. 7a and b), significant values are observed mainly over the tropical and subtropical latitudes. This is probably linked to the strong SST anomaly in the tropical Atlantic in May off the west coast of Africa (Fig. 1b). In the extratropics, the response is weak and not as statistically significant as that simulated in spring. In the North Atlantic and adjacent areas, the responses of the two models agree with each other rather well. Both have a positive height anomaly over the northeast of North America, a wave train response across the North Atlantic to central Europe, with a negative height anomaly over the central Atlantic, a positive anomaly near the UK and a negative center to the east.

The linear regression of the NCEP seasonal mean atmospheric circulation in summer (JJA) to the PC of

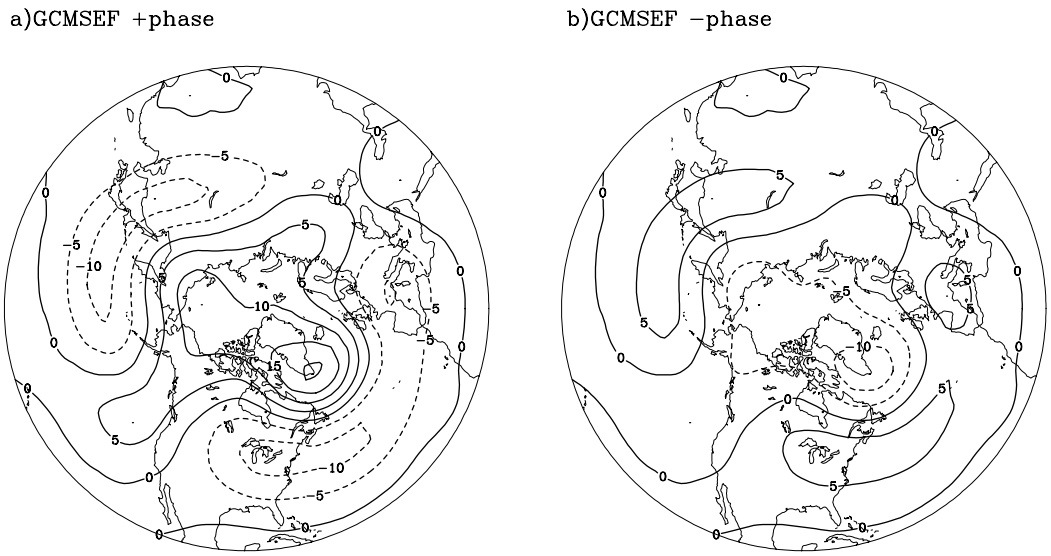

Fig. 6. Composites of MAM 500 hPa height for the years with principal component of EOF 1 of February SST: (a) positive, (b) negative. The contour interval is 5 m.

the same mode of the Atlantic SST anomaly in this season is shown in Fig. 7c. In the extratropics, though statistically not so significant, the main features simulated by the two models shown above also appear, i.e. a positive height anomaly over the northeast of North America, and a wave train across the North Atlantic to central Europe. The SEF model also captures the positive height anomaly over central Russia. The agreement between the two models, however, is poorer than that seen in MAM, and so is the agreement of the models with observations. We will quantify these differences after presenting the results for fall and winter.

5.3. Fall

The results for SON, for which the SST pattern of Fig. 1c is used, are shown in Fig. 8. Again there are similarities in the responses of the two models, especially over the North Atlantic. A positive height anomaly can be found in both models in the southwestern Atlantic and southeastern North America, although weak in the GCM2. In both models a dipole that projects onto the positive NAO is evident, although in both models only part of it is significant at the 5% level.

The observed 500 hPa geopotential SON height anomaly, related to a positive phase of the same mode of the Atlantic SST anomaly, is illustrated in Fig. 8c. Except for the tropics, the observed 500 hPa height anomaly is generally weak, especially over the North Atlantic, and quite different from both model responses.

5.4. Winter

The results for DJF in Fig. 9 show that the two models respond in quite different ways to the same North Atlantic SST anomaly. The response of the SEF is a significant wave train pattern, with a positive height anomaly to the east of the SST heat source, with a maximum value of about 15 m. This pattern is very similar to that observed by Palmer and Sun (1985) with a model forced by a positive SST anomaly in the North Atlantic, and to the November case in Peng et al. (1996). The GCM2 response, on the other hand, is very different. At 500 hPa, the height anomaly has only a weak negative area in the eastern Atlantic. The winter atmospheric response to the SST anomaly in the North Atlantic is clearly highly model-dependent.

The observed pattern (Fig. 9c) is somewhat similar to a positive phase of the NAO. The negative height anomaly near the North Pole reaches about 28 m, and the positive anomaly center over the eastern North Atlantic reaches about 26 m. The DJF seasonal mean temperature field (not shown) has a warm anomaly

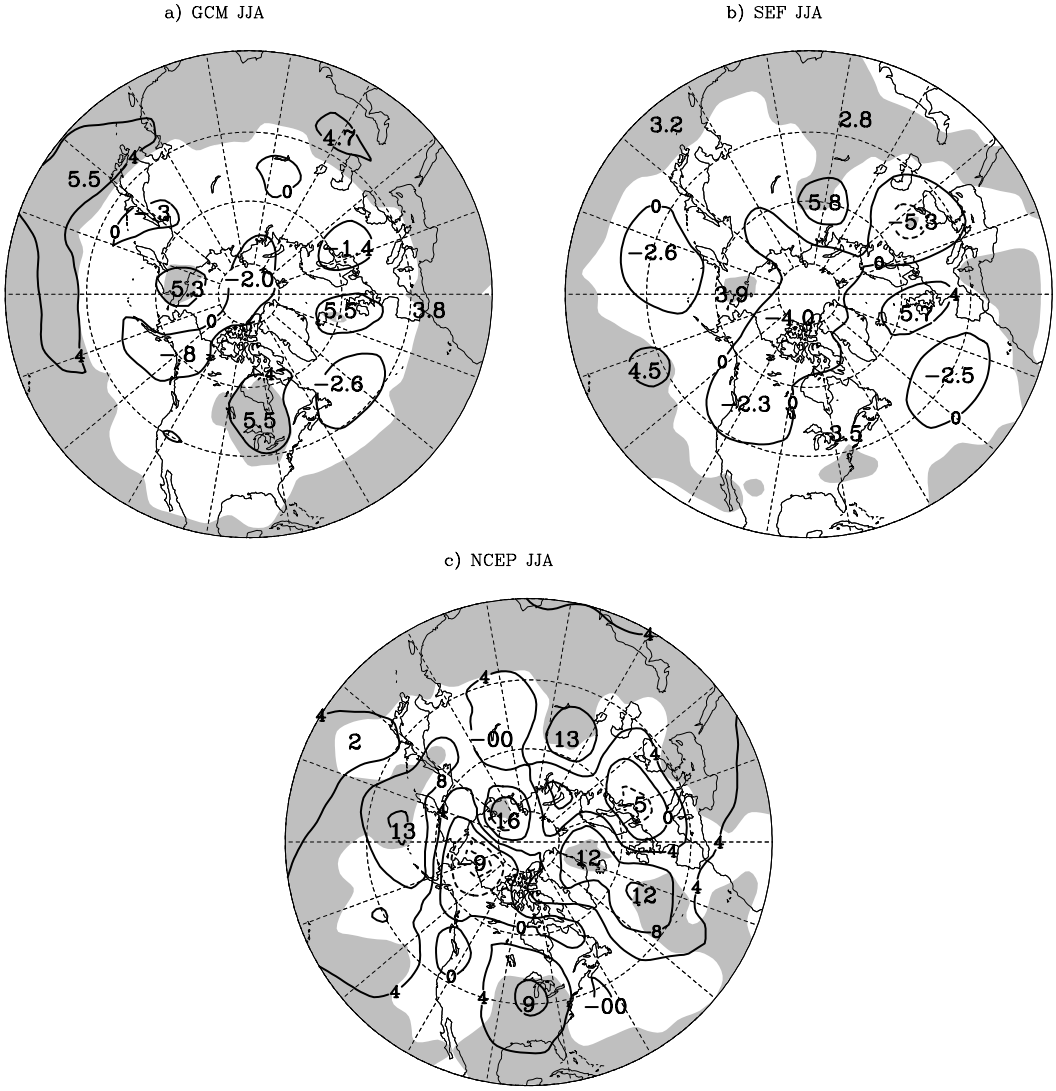

Fig. 7. As Fig. 4 except for summer (JJA).

over Europe all the way to the east coast of Asia, reminiscent of the observed positive NAO (Hurrell, 1995) and AO (Thompson and Wallace, 1998). Both models fail to reproduce this observed atmospheric pattern.

To quantify the above comparison of the model and observed results, Table 1 shows the pattern correlations between the regression anomalies for the NCEP observations and the two models for each season over the region 20–90°N, 90W–90°E. The agreement between the patterns obtained with the NCEP observations and the two models is seen to reach a maximum in MAM, with a correlation coefficient of 0.68 for the NCEP–SEF pair and 0.66 for the NCEP–GCM2 pair. Next to MAM is JJA, with correlation coefficients of 0.37 and 0.31 for the NCEP–SEF and NCEP–GCM2 pairs, respectively. For SON and DJF, the agreement is poor. Except for DJF, the agreement between the two models is good, reaching a remarkable 0.88 in MAM, but we note that the models agree better with each other

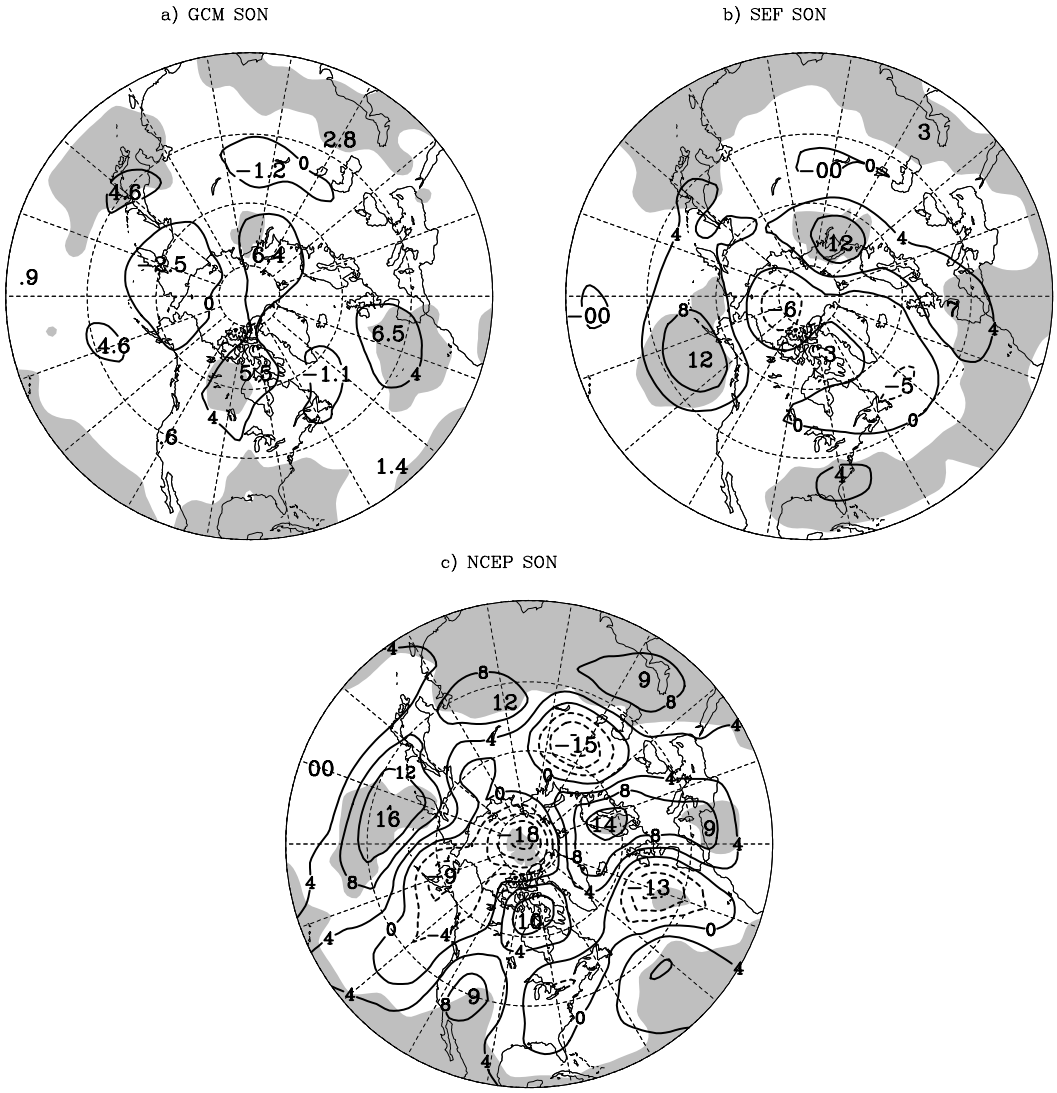

Fig. 8. As Fig. 4 except for fall (SON).

than with observations. The generally good agreement between the two models is related in part to the fact that they use exactly the same specified time-independent SST anomaly in their integrations throughout the season, whereas the atmosphere "sees" a different, time-evolving SST. The atmosphere also has other lower boundary forcing, such as soil conditions, which are absent in the models (see Derome et al., 2001). This adds, of course, another source of discrepancy between the models and the atmosphere. It is interesting to see that in DJF even though the two models use the same specified SST anomaly, their responses are uncorrelated. This suggests that winter is likely to be the most difficult season in which to simulate the atmospheric response to Atlantic SST anomalies. The reason for this is an open question, but one may speculate that the transient eddy feedback may be more important in winter, and difficult to reproduce. The weaker DJF response of the lower-resolution GCM2 (T32) compared to the SEF model (T63) is consistent with this

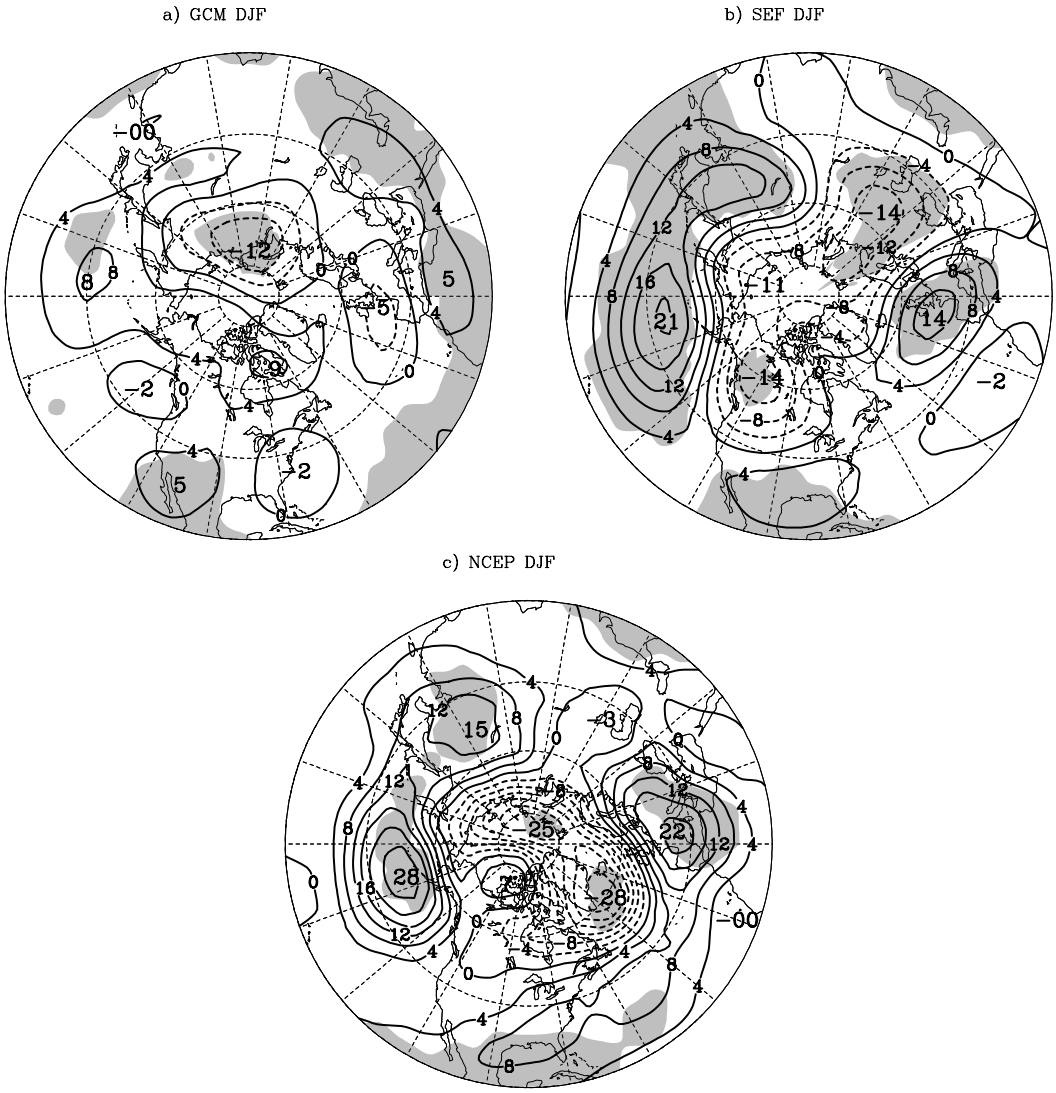

Fig. 9. As Fig. 4 except for winter (DJF).

speculation. Unfortunately, the model output were only available in the form of monthly means, which precluded an analysis of the influence of the transient eddies.

6. Summary and discussion

The Historical Seasonal Forecasting Project (HFP) provides a rich database to study the atmospheric response to specified SST anomalies. In this paper, its output is used to analyze the influence of North Atlantic SST anomalies on seasonal forecasts for each of the four seasons. The atmospheric response to SST anomalies in the North Atlantic is also investigated.

The leading mode of North Atlantic SST of the HFP is identified using an EOF analysis for each of the four seasons. The atmospheric responses to this SST mode are captured by a linear regression analysis. The results show that spring is the season with the best

Table 1. *Pattern correlation between regression maps*

	MAM	JJA	SON	DJF
NCEP−GCM2	0.66	0.31	0.05	−0.01
NCEP−SEF	0.68	0.37	0.16	0.34
GCM2−SEF	0.88	0.55	0.61	0.15

agreement between the responses of the two models used in the HFP, and between the model responses and observations. For the other three seasons notable differences exist between the model responses and the observations.

In a recent study, Peng et al. (2002) produced large ensembles of GCM experiments in a study of the atmospheric response to a North Atlantic SST tripole anomaly. They found that only in February–April does the SST anomaly produce a strong NAO pattern. They related this seasonal dependence to the model's internal variability and to the strong NAO projection of the forced response onto the leading mode in these months. From a different approach, the present study also shows that the SST tripole anomaly in the North Atlantic generates a significant NAO-like pattern in spring. The response is nearly the same for the two models used. In another study, Rodwell and Folland (2002) analyzed 1948–1998 observational data, and their model results suggest some atmospheric seasonal predictability based on a knowledge of preceding North Atlantic SSTs. Their SVD analysis of February monthly mean SST and MAM seasonal mean Z500 reveals a tripole SST pattern and atmospheric NAO response that is very similar to our result.

In spring, summer and fall, the two models agree better with each other than with the observations. In winter the two model responses are radically different. The model-dependence of the results in winter may explain in part why previous studies based on winter data yielded inconclusive results for the atmospheric response to a North Atlantic SST anomaly.

7. Acknowledgements

This research was supported by the Canadian Institute for Climate Studies, the Natural Sciences and Engineering Research Council of Canada and the Canadian Foundation for Climate and Atmospheric Sciences, through the Canadian CLIVAR Research Network.

REFERENCES

Boer, G. J., McFarlane, N. A., Laprise, R., Henderson, J. D. and Blanchet, J.-P. 1984. The Canadian Climate Centre spectral atmospheric general circulation model. *Atmosphere–Ocean* **22**, 397–429.

Branstator, G. 1985. Analysis of general circulation model sea surface temperature anomaly simulations using a linear model. Part I: Forced solutions. *J. Atmos. Sci.* **42**, 2225–2241.

Cassou, C. and Terray, L. 2001. Dual influence of Atlantic and Pacific SST anomalies on the North Atlantic–Europe winter climate. *J. Geophy. Lett.* **28**, 3195–3198.

Cayan, D. R. 1992. Latent and sensible heat flux anomalies over the Northern Oceans: driving the sea surface temperature. *J. Phys. Oceanogr.* **22**, 859–881.

Czaja, A. and Frankignoul, C. 1999. Influence of the North Atlantic SST anomalies on the atmospheric circulation. *J. Geophys. Lett.* **26**, 2969–2972.

Czaja, A. and Frankignoul, C. 2002. Observed impact of Atlantic SST anomalies on the North Atlantic Oscillation. *J. Climate* **15**, 606–623.

Derome, J., Brunet, G., Pante, A., Gagnon, N., Boer, G. J., Zwiers, F. W., Lambert, S. J., Sheng, J. and Ritchie, H. 2001. Seasonal predictions based on two dynamical models. *Atmosphere–Ocean* **39**, 485–501.

Deser, C. and Timlin, M. S. 1997. Atmosphere–ocean interaction on weekly timescales in the North Atlantic and Pacific. *J. Climate* **10**, 393–408.

Ferranti, L., Molteni, F. and Palmer, T. N. 1994. Impact of localized tropical and extratropical SST anomalies in ensembles of seasonal GCM integrations. *Quart. J. R. Meteorol. Soc.* **120**, 1613–1645.

Frankignoul, C. 1985. Sea surface temperature anomalies, planetary waves and air–sea feedbacks in the middle latitude *Rev. Geophys.* **23**, 357–390.

Hall, N. M., Derome, J. and Lin, H. 2001. The extratropical signal generated by a midlatitude SST anomaly. Part I: Sensitivity at equilibrium. *J. Climate* **14**, 2035–2053.

Horel, J. D. and Wallace, J. M. 1981. Planetary scale atmospheric phenomena associated with the Southern Oscillation. *Mon. Wea. Rev.* **109**, 813–829.

Hoskins, B. J. and Karoly, D. J. 1981. The steady linear response of a spherical atmosphere to thermal and orographic forcing. *J. Atmos. Sci.* **38**, 1179–1196.

Hurrell, J. W. 1995. Decadal trends in the North Atlantic Oscillation: regional temperature and precipitation. *Science* **269**, 676–679.

Kalnay, E., Kanamitsu, M., Kistler, R., Collins, W., Deaven, D., Gandin, L., Iredell, M., Saha, S., White, G., Woolen,

J., Zhu, Y., Chelliah, M., Ebisuzaki, W., Higgins, W., Janowiak, J., Mo, K. C., Ropelewski, C., Wang, J., Leetmaa, A., Reynolds, R., Jenne, R. and Joseph, D. 1996. The NCEP/NCAR 40-year reanalysis project *Bull. Am. Meteorol. Soc.* **77**, 437–471.

Kumar, A. and Hoerling, M. P. 1995. Prospects and limitations of atmospheric GCM climate predictions. *Bull. Am. Meteorol. Soc.* **76**, 335–345.

Kushnir, Y. 1994. Interdecadal variations in north Atlantic Sea surface temperature and associated atmospheric conditions. *J. Climate* **7**, 141–157.

Kushnir, Y. and Held, I. M. 1996. Equilibrium atmospheric response to North Atlantic SST anomalies *J. Climate* **9**, 1208–1220.

Kushnir, Y. and Lau, N.-C. 1992. The general circulation model response to a North Pacific SST anomaly: dependence on time scale and pattern polarity. *J. Climate* **5**, 271–283.

Lau, N.-C. and Nath, M. J. 1990. A general circulation model study of the atmospheric response to extratropical SST anomalies observed in 1950-79. *J. Climate* **3**, 965–989.

Lau, N.-C. and Nath, M. J. 1994. A modeling study of the relative roles of tropical and extratropical SST anomalies in the variability of the global atmosphere–ocean system. *J. Climate* **7**, 1184–1207.

McFarlane, N. A., Boer, G. J., Blanchet, J.-P. and Lazare, M. 1992. The Canadian Climate Centre second-generation general circulation model and its equilibrium climate. *J. Climate* **5**, 1013–1044.

Palmer, T. N. and Sun, Z. 1985. A modelling and observational study of the relationship between sea surface temperature in the northwest Atlantic and atmospheric general circulation. *Quart. J. R. Meteorol. Soc.* **111**, 947–975.

Peng, S. and Whitaker, J. S. 1999. Mechanisms determining the atmospheric response to midlatitude SST anomalies. *J. Climate* **12**, 1393–1408.

Peng, S., Mysak, L. A., Ritchie, H., Derome, J. and Dugas, B. 1995. The differences between early and midwinter responses to sea surface temperature anomalies in the northwest Atlantic. *J. Climate* **8**, 137–157.

Peng, S., Robinson, W. A. and Hoerling, M. P. 1997. The modeled atmospheric response to midlatitude SST anomalies and its dependence on background circulation states. *J. Climate* **10**, 971–987.

Peng, S., Robinson, W. A. and Li, S. 2002. North Atlantic SST forcing of the NAO and relationships with intrinsic Hemispheric variability. *Geophys. Res. Lett.* **29**, 117.

Pitcher, E. J. 1988. Effect of North Pacific sea surface temperature anomalies on the January climate of a general circulation mode. *J. Atmos. Sci.* **45**, 173–188.

Rayner, N. A., Horton, E. B., Parker, D. E., Folland, C. K. and Hackett, R. B. 1996. Version 2.2 of the global sea-ice and sea surface temperature data set, 1903–1994. *Climate Research Technical Note no. 74*, Hadley Centre, UKMO, Bracknell, UK.

Ritchie, H. 1991. Application of the semi-Lagrangian method to a multilevel spectral primitive-equation model. *Quart. J. R. Meteorol. Soc.* **117**, 91–106.

Ritchie, H. and Beaudoin, C. 1994. Approximation and sensitivity experiments with a baroclinic semi-Lagrangian spectral model. *Mon. Wea. Rev.* **122**, 2391–2399.

Rodwell, M. J. and Folland, C. F. 2002. Atlantic air-sea interaction and seasonal predictability. *Quart. J. R. Meteorol. Soc.* **128**, 1413–1443.

Robertson, A. W., Mechoso, C. R. and Kim, Y. J. 2000. The influence of Atlantic sea surface temperature anomalies to the North Atlantic Oscillation. *J. Climate* **13**, 122–138.

Robinson, W. A. 2000. Review of WETSthe workshop on extra-tropical SST anomalies. *Bull. Am. Meteorol. Soc.* **81**, 567–577.

Thompson, D. W. J. and Wallace, J. M. 1998. The Arctic Oscillation signature in the wintertime geopotential height and temperature fields. *Geophys. Res. Lett.* **25**, 1297–1300.

Zwiers, F. W. 1996. Interannual variability and predictability in an ensemble of AMIP climate simulations conducted with CCC GCM2. *Climate Dynam.* **12**, 825–847.